

NUMERICAL SIMULATION OF THE NATURAL CONVECTION IN VERTICAL CHANNELS CONTAINING PROTRUDING HEAT SOURCES WITH AN UNHEATED ENTRY OR UNHEATED EXIT

Ana Cristina Avelar

ASA-L / IAE / CTA
cristi@directnet.com.br

Marcelo Moreira Ganzarolli

DE / FEM / UNICAMP
ganza@fem.unicamp.br

Abstract. *In the present study, numerical simulations were performed to investigate the partial heating of the plates in an array of vertical channels with protruding heat sources cooled by natural convection. The configurations considered included an unheated region from the entrance and from the exit of the channel, and the uniform heating of the plates. A parametric analysis was performed by varying the length of the unheated region, the distance between plates, and the power dissipated per plate. A two-dimensional mathematical model based on the conservation equations of mass, momentum and energy, including heat conduction to the walls was adopted. The numerical solutions were carried out using a finite volume discretization and the SIMPLER algorithm for solving the pressure-velocity coupling. Comparison of numerical results with experimental data showed a good agreement between them. It was observed that the uniform heating of the channels led to the lowest temperature values and the highest values occurred in the configuration with the entrance regions of the channels not being heated.*

Keywords. *Natural Convection, Vertical Channels, Unheated, Non-uniform heating, Protruding heat sources.*

1. Introduction

Natural convection heat transfer in vertical channels has been intensively investigated in the last decade because of its application in various thermal systems, such as electronic components, ventilation systems, solar energy systems and others. Free convection is an attractive cooling process because of its simplicity, low cost and reliability. In addition, this process constitutes the only mechanism capable of transferring heat from a plate to a coolant in case of power failure of devices that sustain forced convection flows.

Nowadays, the majority of the studies about natural convection, with application in thermal design of cooling of electronic components, are seeking for new configurations to enhance the heat transfer parameters or the optimization of standard configurations (Auletta et al, 2001). In this context, the concept of partial heating has been explored in some publications. The placement of adiabatic extensions downstream of the heated channels is one of the techniques employed to improve the heat transfer rate. This configuration induces an increment of the flow rate due to the well-known "chimney effect". Haaland and Sparrow (1983) were the first researchers to show that a higher flow rate of fluid through a confined open-ended enclosure can be induced by the chimney effect. They carried out a numerical investigation for natural convection flow in a vertical channel with a point heat source (channel plume problem) or distributed heat sources situated at the channel inlet (chimney problem). Wirtz and Haag (1985) obtained experimental results for symmetric isothermal heated plates with an attached unheated entry portion. Their investigation was carried out over a wide range of Rayleigh Numbers, from the single-plate limit to the fully developed flow. They found that the flow is quite insensitive to the presence of the unheated entry section for large channel spacing, while it is severely affected when the gap spacing is small. Lee (1994) analyzed numerically channels formed by isothermal or isoflux plates with unheated extensions placed near the entrance or the exit of the channels. The boundary layer approximation was used in the analysis. Campo et al (1999) reformulated the problem analyzed by Lee (1994) using the elliptic model for the conservation equations. Autella et al. (2001) investigated the effect of adding extensions downstream of a vertical, isoflux and symmetrically heated channel. Optimal configurations were identified by measuring the wall temperature profiles variation with the length and expansion ratios of the insulated extensions. In addition, there are several studies dealing with channels with protruding heat sources, with the objective of improving the heat transfer rates. Fujii et al (1996) analyzed numerical and experimentally the natural convection heat transfer to air from an array of vertical parallel plates with protruding, discrete and densely distributed, heat sources. A thermal optimum spacing of the parallel plates was also discussed in this work. Behind and Nakayama (1998) performed numerical simulations on natural convection considering the same geometry analyzed by Fujii et al (1996), but the analysis was performed for several values of substrate thermal conductivity and channel width. Bessaih and Kadja (2000) carried out numerical simulations on turbulent natural convection cooling of three identical heated ceramic components mounted on a vertical

adiabatic channel wall. It was investigated the effect of the spacing between components and of the removal of heat input in one of the components. The conjugated conduction-convection heat transfer problem in an array of vertical open channels with heated protruding heat sources was numerically and experimentally investigated by Avelar and Ganzarolli (2002). Uniform and non-uniform heating of the plates was analyzed. Both the distance between plates and power dissipated per plate were varied. In the non-uniform heating conditions one heat-source was electrically fed with a different power level from the others, and the influence of the location of this element on the temperature distribution was investigated. This work was extended by Avelar and Ganzarolli (2003) with the calculation, for the uniform heating condition, of an optimum spacing between plates that maximizes the dissipation, per unit volume, for a prescribed temperature in a stack of parallel plates cooled by natural convection. The purpose of the present paper is to extend the previous works of Avelar and Ganzarolli (2002, 2003) by investigating the partial heating of the plates when some heat-sources, near the entrance or near the exit of the channel, are non-powered. The length of this unheated region, i.e. the number of non-powered elements, the distance between plates, and the power dissipated per plate were varied. It was analyzed the effect of the partial heating in the mass flow rate induced into the channels and in the temperature distribution along them. Numerical solutions were obtained to the full elliptic two-dimensional steady-state equations of continuity, momentum and energy, including heat conduction to the walls, using a finite volume discretization and the SIMPLEC algorithm for pressure-velocity coupling. Comparisons of numerical results with experimental data showed a good agreement between them. Comparing the heating conditions investigated, it was verified that the lowest values of maximum temperature in the plates were found for the uniform heating conditions, followed by the case when three protruding heat sources were left non-powered in the channel exit.

2. Numerical simulation

Figure (1) shows the physical array of the channels and the coordinate system used. The model assumes an infinite number of plates placed in a vertical parallel arrangement with equal spacing, d , between plates. The plates have the same length, l and thickness, b . On one side of the plates seven two-dimensional protruding heat sources of the same dimensions are mounted, separated by the distance, s . The heating configuration is set to be the same in all the plates which leads to a periodic behavior. Hence, the solution domain can be represented by a single channel, identified in Fig. (1) by the dashed line.

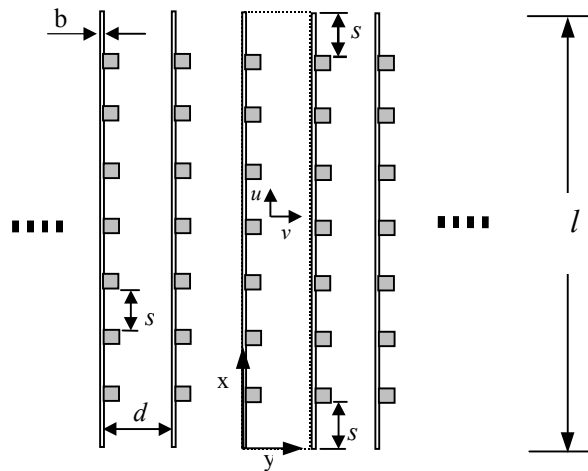


Figure 1 – Physical array and coordinate system.

The flow is assumed to be at steady state, laminar and two-dimensional. The air thermo-physical properties are assumed to remain constant, except for the density in the buoyancy term of the momentum equation, for which the Boussinesq approximation is adopted. The heat conduction in the plates and in the heat sources is also taken into account, with a uniform heat generation within the heat sources. Radiation heat transfer is not considered. The problem is analyzed for the situations of uniform and non-uniform heating of the plates. In the case of non-uniform heating, the partial heating of the channels is investigated. The governing equations are expressed in dimensionless form as follow:

Continuity equation

$$\frac{\partial U}{\partial X} + \frac{\partial V}{\partial Y} = 0 \quad (1)$$

Momentum equation in X direction

$$U \frac{\partial U}{\partial X} + V \frac{\partial U}{\partial Y} = -\frac{\partial P}{\partial Y} + \left(\frac{\text{Pr}}{\text{Ra}}\right)^{1/2} \left(\frac{\partial^2 U}{\partial X^2} + \frac{\partial^2 U}{\partial Y^2}\right) + \theta \quad (2)$$

Momentum equation in Y direction

$$U \frac{\partial V}{\partial X} + V \frac{\partial V}{\partial Y} = -\frac{\partial P}{\partial Y} + \left(\frac{\text{Pr}}{\text{Ra}}\right)^{1/2} \left(\frac{\partial^2 V}{\partial X^2} + \frac{\partial^2 V}{\partial Y^2}\right) \quad (3)$$

Energy equation

$$U \frac{\partial \theta}{\partial X} + V \frac{\partial \theta}{\partial Y} = \left(\frac{\text{Pr}}{\text{Ra}}\right)^{1/2} \frac{k_i}{k_{air}} \left(\frac{\partial^2 \theta}{\partial X^2} + \frac{\partial^2 \theta}{\partial Y^2}\right) + f x S^* \quad (4)$$

The dimensionless variables in the above equations are defined by

$$\begin{aligned} X &= \frac{x}{d}, \quad Y = \frac{y}{d}, \quad L = \frac{l}{d}, \quad B = \frac{b}{d} \\ \theta &= \frac{T - T_i}{q'' d / k_{air}}, \quad U = \frac{u}{u_o}, \quad V = \frac{v}{u_o}, \quad P = \frac{p - p_h}{\rho u_o^2} \\ \text{Ra} &= \frac{q'' d^4 \beta}{k_{air} \nu_{air} \alpha_{air}}, \quad \text{Pr} = \frac{\nu}{\alpha} \end{aligned} \quad (5)$$

where T_i is the air temperature at the channel inlet, p_h is the hydrostatic reference pressure in the channel and q'' is defined based on the total surface area of the plate, A , and the total heat generation per plate, Q , as

$$q'' = \frac{Q}{2A} \quad (6)$$

The reference velocity, u_o is defined by

$$u_o = \left(d^2 g \beta \frac{q''}{k_{air}} \right)^{1/2} \quad (7)$$

In the energy equation, Eq. (4), the following apply:

- $f = 1$ for the protruding heat sources and $f = 0$ for the rest of the domain;
- k_i is thermal conductivity of the correspondent region. $i = 1, 2$ and 3 , for air, plate and heating sources, respectively;
- The source term S^* , depends on the configuration being given by

$$S^* = \frac{2L}{n_h \times XPT \times YPT \times \sqrt{\text{PrRa}}} \quad (8)$$

where n_h is the number of powered heat sources and XPT and YPT are the dimensionless protruding element dimensions.

The boundary conditions are:

$$\text{Channel entrance } (X = 0): \theta = V = 0; P = -0.5 U_m^2 \quad (9)$$

where U_m is the mean velocity in the channel.

$$\text{Channel Walls } (Y = 0 \text{ and } Y = B + 1): U = V = 0; \theta(X, 0) = \theta(X, B + 1) \quad (10)$$

Channel exit ($Y = l/d$):

$$\frac{\partial U}{\partial X} = \frac{\partial V}{\partial X} = \frac{\partial \theta}{\partial X} = P = 0 \quad (11)$$

The pressure values at the channel entrance and exit, Eq. (6) and Eq. (8), were obtained considering potential flow. Eq. (7) represent the non-slip condition at the channel walls and the periodicity of temperature.

The governing equations are discretized using the control volume formulation with the power-law interpolation of convective terms, as described by Patankar (1980). The velocity control volumes are staggered with respect to the pressure and temperature control volumes and the coupling of pressure and velocity fields is treated using the SIMPLEC (SIMPLE-Consistent) algorithm (Van Doormal and Raithby, 1984). The SIMPLEC follows the same steps as the SIMPLE algorithm of Patankar and Spalding (1972), with the difference that the momentum equations are manipulated so that the velocity correction equations omit terms that are less significant than those omitted in SIMPLE. The conjugate conduction-convection heat transfer is treated by using the harmonic mean of thermal conductivity at the solid-fluid interfaces, as described in Patankar (1980). The periodic boundary condition imposed with respect to the temperature at the plate surfaces is handled by using the CTDMA (Cyclic TriDiagonal Matrix Algorithm) algorithm, from Patankar et al. (1977), to solve the discretized energy equation.

The implementation of the prescribed pressure value at the ends of the channel was carried as suggested by Versteeg and Malalasekera (1995). Pressure values were imposed at the nodes just inside the physical boundary, as indicated in Fig. (2) and Fig. (3) by solid circles. The pressure corrections (p') were set to zero in these nodes.

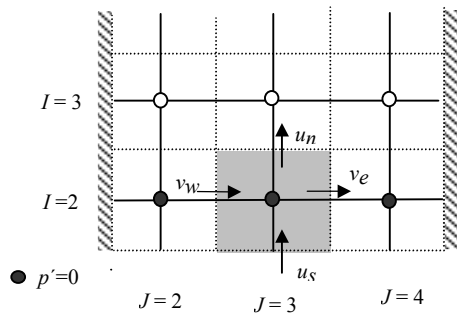


Figure 2 - p' -cell at the channel inlet.

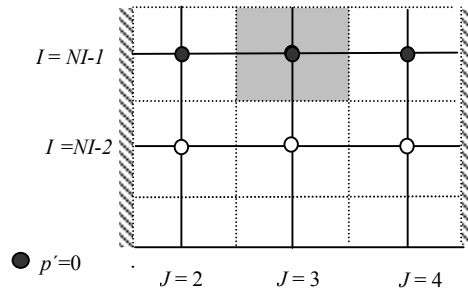


Figure 3 - p' -cell at the channel outlet.

The u -velocity components across the domain boundary is generated as part of the solution process by ensuring that continuity is satisfied at every cell. For example, in Fig. 2 the values of u_s , v_e and v_w emerge from solving the discretised u - and v - momentum equations inside the domain. Given these values it is possible to compute the velocity in the channel entrance, u_s , by mass conservation in the for the $p'=0$ cell. This yields

$$u_s = \frac{(\rho u A)_n + (\rho v A)_e - (\rho v A)_w}{(\rho A)_s} \quad (12)$$

thus, the air velocity in the channel entrance is computed as part of numerical solution.

The equations are solved in a non-uniform grid with a greater refinement near the solid walls. The number of nodes is varied from 622~56 to 622~64, depending on the distance between plates. The grid distributions were determined by successive refinements of an initial 312~26 grid until the maximum temperature in the plate changes were below 1%. The convergence of the numerical procedure was tested by the following criterion

$$\frac{|\Gamma_{i,j}^n - \Gamma_{i,j}^{n-1}|_{max}}{|\Gamma_{i,j}^n|_{max}} \leq 5.0 \times 10^{-6} \quad (13)$$

where Γ stands for U , V , θ and the maximum residue in the continuity equation.

3. Experimental Apparatus

The experimental apparatus used was the same described in the previous works of Avelar and Ganzarolli (2002, 2003). An array of five fiber glass plates, each one with 365mm height (l), 340mm width (w) and with 1.5mm

thickness, and with seven heat sources mounted on its surface was accommodated in a structure that allows variation of the distance between plates. The protruding heat sources were constructed from two aluminum bars 12.25mm height, 340mm width and 6.13mm thickness, with one resistance wire inserted between them. The resulting elements were screwed into the fiber glass plates and an equal spacing of 34.5mm was adopted. The protruding heat sources were connected in a way that any desired power level could be set to any given element, independently of the others. Power was supplied to the plates by regulated D.C. sources and both sides of the channels were closed to prevent lateral air flowing. In order to reduce the radiation heat transfer influence, the heat sources were polished with diamond paste. The structure was maintained about 1m from the ground and placed in a quiet room. Temperature measurements were obtained by using calibrated thermocouples 36 AWG type J, a switch and a digital thermometer. Special care was taken to embed the thermocouples in the aluminum and in the fiber glass surfaces. A very small hole was drilled in their surfaces, which was covered with a thin layer of thermal paste, and the thermocouples were fixed with epoxy adhesive.

The hypotheses of two-dimensionality, periodicity of temperature and negligible contact resistance, used in the numerical model, were verified to be valid for the central plate of the experimental apparatus. Hence, the temperature values measured on the heat sources of the central plate of the arrangement could be used for validation of the numerical results.

In Fig. (4) it is schematically presented the heating configurations investigated in this study. For convenience, the protruding heat sources were numbered from 1 to 7. The number 1 corresponding to the element placed near the channel inlet, and number 7 to the element placed near the channel outlet. As indicated in the Fig. (4), the total power dissipated per plate was maintained constant in all the cases analyzed.

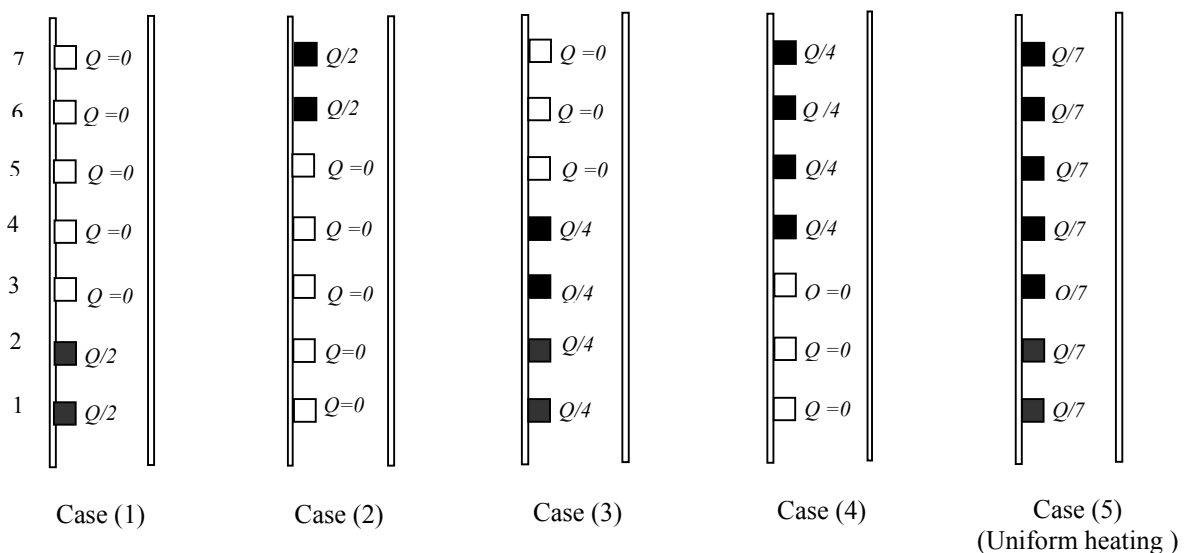


Figure 4 – Partial heating cases investigated.

Experiments and numerical simulations were run various distances between plates and total heat generation rates, Q , which was set to be the same for all plates during the tests. The distance between plates was varied from 2.0 to 4.5cm, which corresponds to aspect ratios ($L = l/d$) between 9.0 and 18.0, and the total heat generation per plate from 10 to 30W, corresponding to Rayleigh number values ranging from 2.0×10^3 to 2×10^4 .

4. Results and discussions

Figure (5a-d) presents numerical results for temperature excess profile for Case (1), Case (2) and Case (5) for a power dissipated per plate of 10W and distances between plates varying from 2.0 to 3.3 cm. The temperature excess is defined as the difference between the protuberances temperature and the air temperature in the channel inlet.

From Fig. (5a-d), it can be observed that the temperature excess value on the protruding heat sources decreases as the distance between plates increases, tending to a value that is not dependent on the distance, i.e., the value correspondent to the limit case of a plate isolated in an infinite medium. In Fig. (5a), it can be noticed that when the plate-to-plate spacing is equal to 2cm, the maximum temperature excess value achieved in Case (2) is considerably higher than in Case (1). It can also be noticed from Fig. (5a-d) that in Case (1), the thermal wake from the upstream elements cause an increase on the downstream elements temperature. This effect is more evident for the smaller distances between plates. These tendencies were also observed for other power dissipated per plate values.

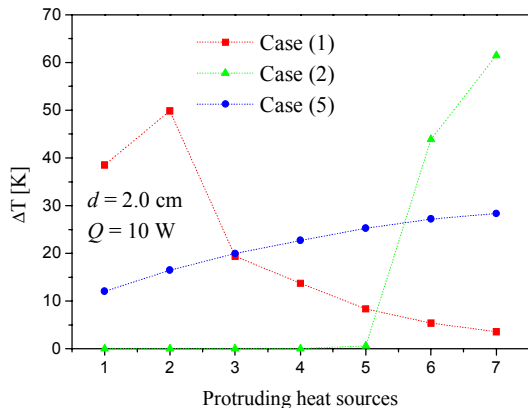


Figure 5a - Numerical temperature profiles $d = 2.0 \text{ cm} - Q = 10 \text{ W}$.

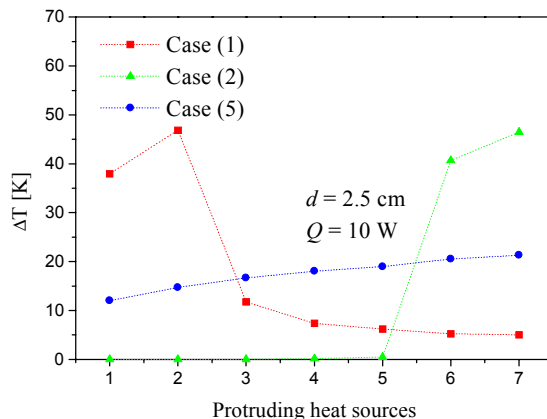


Figure 5b - Numerical temperature profiles $d = 2.5 \text{ cm} - Q = 10 \text{ W}$.

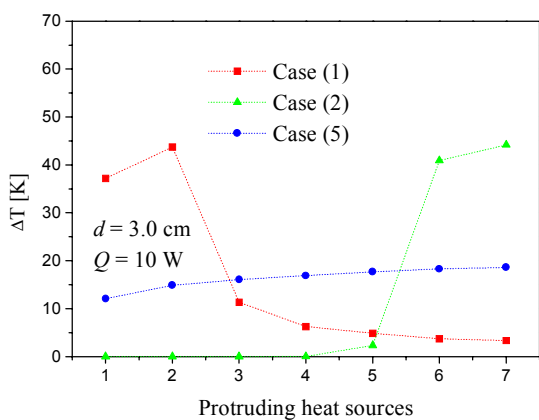


Figure 5c - Numerical temperature profiles $d = 3.0 \text{ cm} - Q = 10 \text{ W}$.

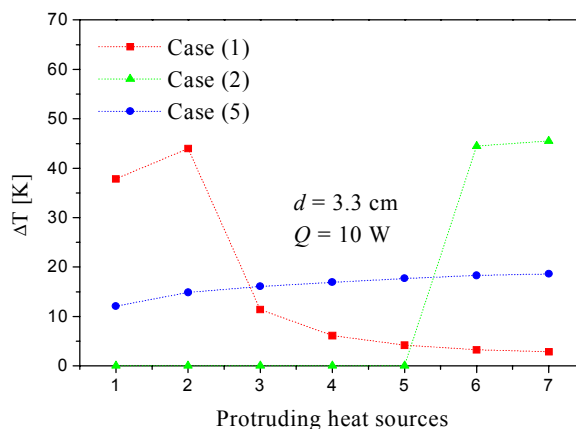


Figure 5d - Numerical temperature profiles $d = 3.0 \text{ cm} - Q = 10 \text{ W}$.

Figure (6) and Fig. (7) show numerical temperature excess profiles for Case (3), Case (4) and Case (5). The results presented in Fig. (6a) and Fig. (6b) are correspondent to the distance between plates of 2.cm and power dissipated per plate of 10 W and 20 W, respectively.

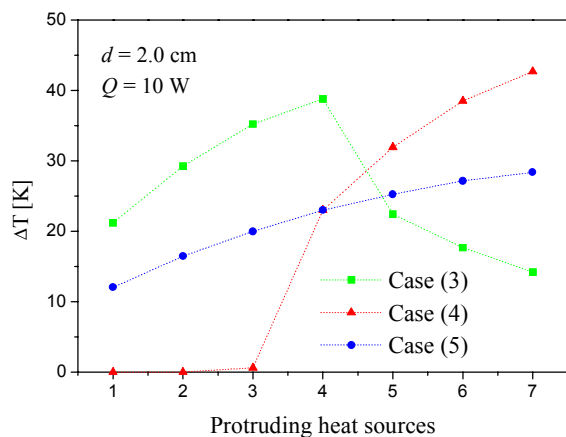


Figure 6a - Numerical temperature profiles $d = 2.0 \text{ cm} - Q = 10 \text{ W}$.

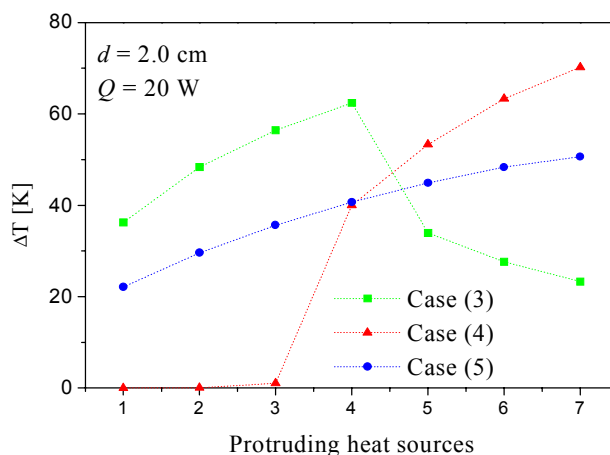


Figure 6b - Numerical temperature profiles $d = 2.0 \text{ cm} - Q = 20 \text{ W}$.

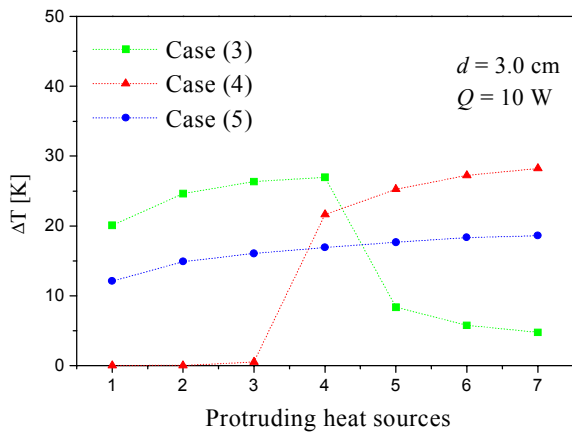


Figure 7 a - Numerical temperature profiles
 $d = 3.0 \text{ cm} - Q = 10 \text{ W}$.

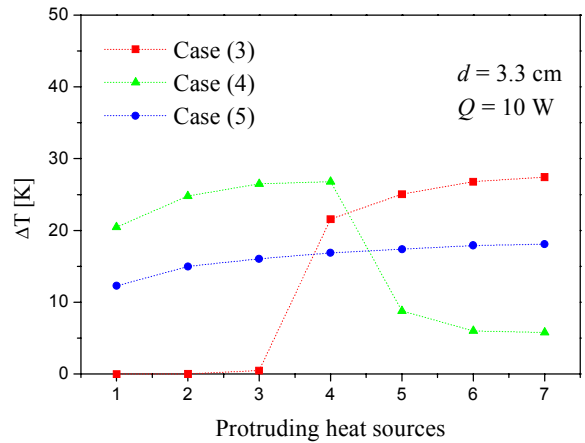


Figure 7 b - Numerical temperature profiles
 $d = 3.0 \text{ cm} - Q = 10 \text{ W}$.

The results presented in Fig. (7a) and Fig (7b) refer to the distances between plates of 3.0 cm and 3.3 cm, respectively, and power of 10W.

Globally, the results from Fig. (6) and Fig. (7) lead to conclusions similar to those from Fig.(5). It can be observed that the temperature excess values tend to the limit case of a plate isolated in an infinite medium, as the distance between plates increases. Similarly to Fig. (5a), Fig. (6a-b) indicate that for the distance of 2cm, the maximum temperature excess value achieved in Case (4) is considerably higher than in Case (3). It can also be noticed that in Case (3), the thermal wake from the upstream elements provoke an increase on the downstream elements temperature, as it was observed in Case (1). In addition, comparing Fig. (6a) and Fig. (6b), it can be noticed that the temperatures excess profiles present only slight variations with the increase in the heat rate dissipated per plate.

Table (1) shows numerical values of channel mean velocity for distance between plates varying from 2.0cm to 3.3cm and total power dissipated per plate equal to 10W.

Table 1 – Channel mean velocity – $Q = 10\text{W}$.

d (cm)	Ra	U (m/s)				
		Case (1)	Case (2)	Case (3)	Case (4)	Case (5)
2.0	2.0×10^3	0.065	0.04	0.075	0.054	0.067
2.5	5.4×10^3	0.10	0.06	0.099	0.08	0.095
3.0	1.0×10^4	0.11	0.063	0.11	0.09	0.107
3.3	1.7×10^4	0.12	0.069	0.12	0.11	0.118

It can be observed from Tab. (1) that for all distances, the channel mean velocity values are very similar in Case (1) and Case (3), where the powered elements are near the channel inlet, and in Case (5). This is a consequence of the “chimney effect” which also makes the flow induced in the channel in Case (1) to be considerably higher than in Case (2). In Case (1) and Case (3), the thermal wake from the elements placed near the channel inlet enhance the global buoyancy in the channel, consequently increasing the mean velocity of the induced flow.

Table (2) shows maximum plate temperature excess values for distance between plates varying from 2.0cm to 3.3cm and total power dissipated per plate equal to 10W.

Table 2 – Plate maximum temperature values – $Q = 10\text{W}$.

d (cm)	Ra	ΔT_{max}				
		Case (1)	Case (2)	Case (3)	Case (4)	Case (5)
2.0	2.0×10^3	49.8	61.47	38.8	42.7	28.34
2.5	5.4×10^3	46.8	47.65	27.2	28.35	20.53
3.0	1.0×10^4	43.7	44.16	26.0	28.0	18.59
3.3	1.7×10^4	43.0	44.0	26.0	26.8	18.0

From Tab. (2) it can be noticed that, for all values of d , the highest value of ΔT_{max} was observed in Case (2), and the lowest values in Case (5). It can also be noticed that for distances above 2.5cm, there is practically no difference, in

terms of ΔT_{max} , between placing the powered heat sources in the channel entrance region, Case (1) and Case (3), and in the exit region Case (2) and Case (4). It can be concluded that, in terms of electronic thermal design, for similar arrangements, the uniform heating is the best option, followed by the placement of heated components near the channel entrance, which is more effective for small distances between plates.

Table (3) shows values of mean velocity in the channel, for all the cases studied, for distance between plates equal to 2.0cm and total power dissipated per plate equal to 10W and 20W.

Table 3 – Mean velocity values in the channel – $d = 2.0$ cm.

Q (W)	Ra	U (m/s)				
		Case 1	Case 2	Case 3	Case 4	Case 5
10	2.0×10^3	0.065	0.04	0.075	0.054	0.067
20	4.0×10^3	0.093	0.056	0.10	0.074	0.094

From the results presented in Tab. (3), it can be noticed that the channel flow increases, in a smaller rate, with the increment of the total power dissipated per plate and the Rayleigh number, as usually expected for channel flows induced by buoyancy forces. The similarity of the mean velocity values in the channel for Case (1), Case (3) and Case (5) can be noticed for both power levels.

Experimental results of temperature excess profiles for Case (1), Case (2) and Case (5) for the distances between plates equal to 2.0 and 2.5 cm and power dissipated per plate of 10W are presented in Fig. (8) and Fig. (9).

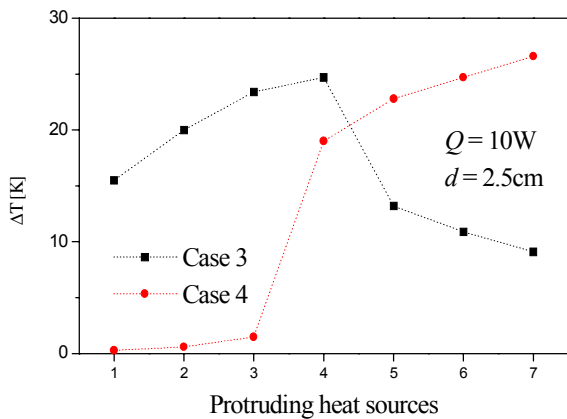


Figure 8 - Experimental temperature profiles $d = 2.5$ cm – $Q = 10$ W.

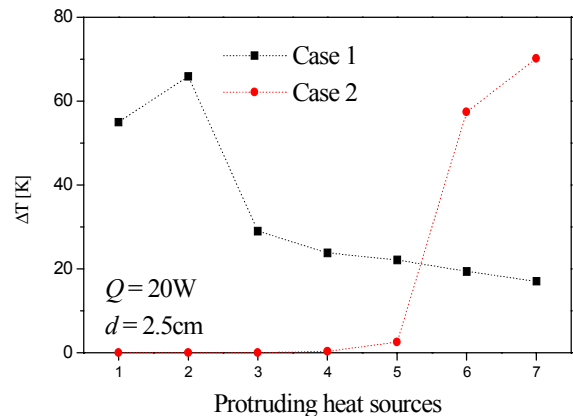


Figure 9 - Experimental temperature profiles $d = 2.5$ cm – $Q = 20$ W.

From Fig. (8) and Fig. (9), it can be noticed that the temperature excess profile experimentally determined was well anticipated by the numerical results. It can also be observed that the highest temperature excess values were verified in the cases with unheated entries, Case (2) and Case (4), which is in agreement with the numerical results.

Figure (10) and Fig. (11) present comparisons between numerical and experimental results of temperature excess values for Case (1) and Case (3), for a distance between plates of 2.5cm and a power dissipated of 20W.

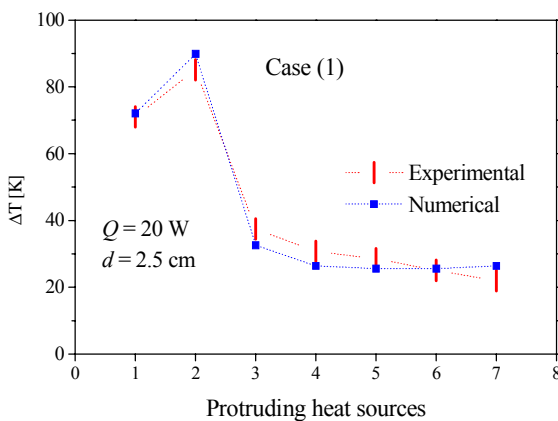


Figure 10 - Temperature profiles $d = 2.5$ cm – $Q = 20$ W.

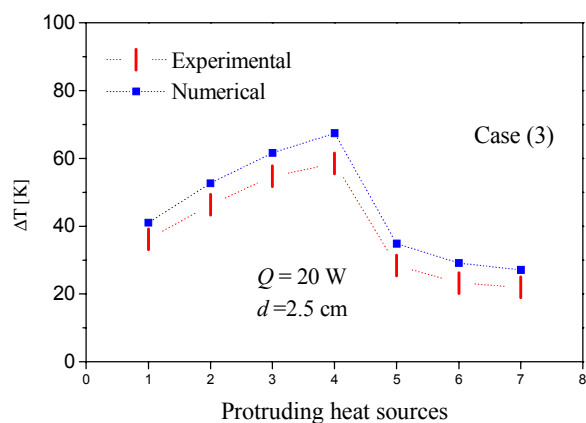


Figure 11 - Temperature profiles $d = 2.5$ cm – $Q = 20$ W.

As can be noted from Fig. (10) and Fig. (11), good agreement between numerical and experimental results was verified, with the largest difference being around 12%.

Figures (12) to (16) present contour plots of dimensionless temperature values for all heating configurations analyzed, with $d=2.5\text{cm}$ and $Q=10\text{W}$. In Fig. (12) it is presented isotherms for Case 5 (the uniform heating) and in Figs. (13) to (16) for the non-uniform heating cases. The channel is displayed in the horizontal direction for convenience.

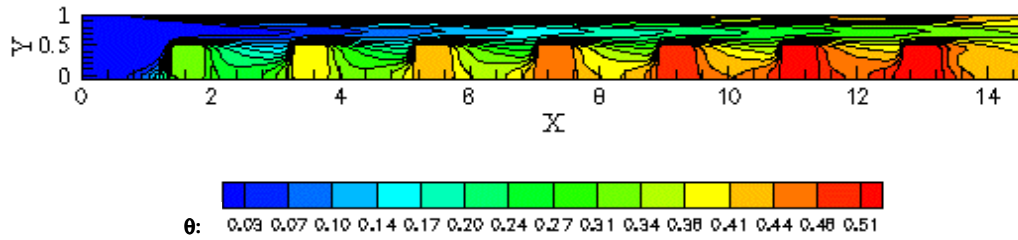


Figure 12 - Isotherms – $d = 2.5\text{cm} - Q = 10\text{W} - \text{Case (5)}$ (uniform heating condition).

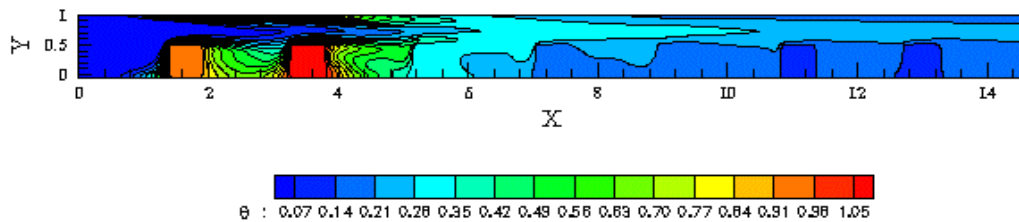


Figure 13 - Isotherms – $d = 2.5\text{cm} - Q = 10\text{W} - \text{Case (1)}$.

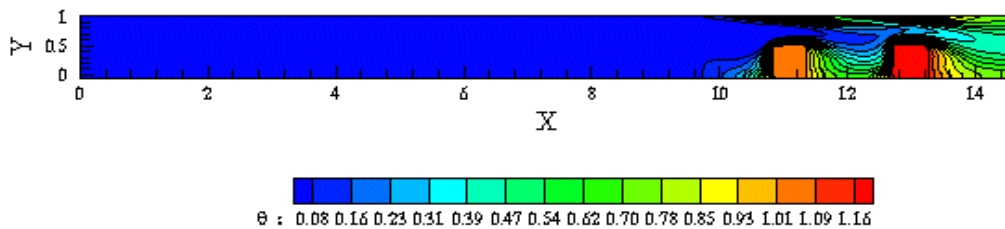


Figure 14 - Isotherms – $d = 2.5\text{cm} - Q = 10\text{W} - \text{Case (2)}$.

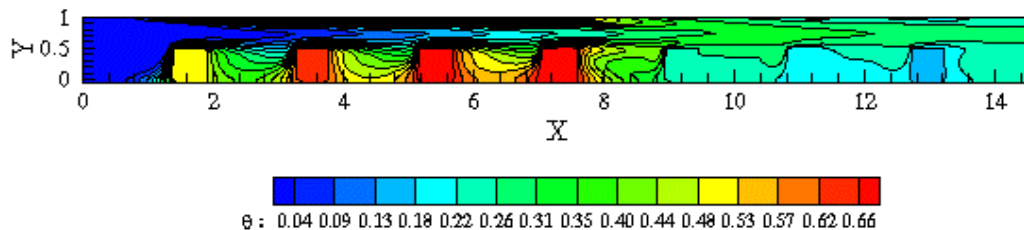


Figure 15 - Isotherms – $d = 2.5\text{cm} - Q = 10\text{W} - \text{Case (3)}$.

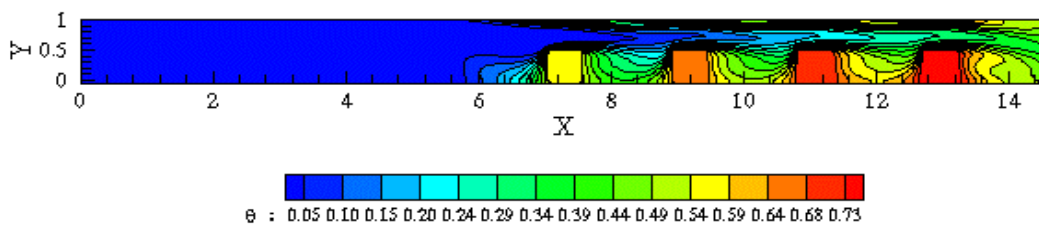


Figure 16 - Isotherms – $d = 2.5\text{cm} - Q = 10\text{W} - \text{Case (4)}$.

From Figs. (12) to (16) it can be noticed that the isothermal lines are crowded on the surfaces that are parallel to the main flow direction and near the protrusions bottom corner, meaning that the heat transfer rates are higher in these regions. It can be observed that in the cases with an unheated entry, the powered elements near the channel exit have

no effect in the upstream elements temperature, which is very near to ambient air temperature. On the other hand, it is possible to perceive the influence of thermal wake in the cases with an unheated exit.

5. Conclusion

In the present work the effect of non-uniform heating in an array of vertical channels with protruding heat sources, cooled by natural convection, was investigated by numerical simulations. The configurations analyzed included an unheated channel entry, an unheated channel exit and the uniform heating condition. A parametric analysis was performed by varying the distance between plates, the length of the unheated region and the power dissipated per plate. The configurations were compared in terms of temperature excess and induced velocities in the channel. The results obtained were shown to be in good agreement with experimental data.

For all configurations, it was observed that the temperature excess values on the protruding heat sources decreased as the distance between plates increased, tending to a value corresponding to a limit case of a single-plate, isolated in an infinite medium. Those conclusions were shown not to be affected by the length of the unheated region or the power dissipated per plate.

Comparing the cases analyzed, the lowest temperature excess values were verified for the uniform heating condition, followed by the configurations where the non-powered heat sources were left near the channel outlet, due to the “chimney effect”. In addition, it was observed that the induced velocity values of the unheated exit cases were very similar to the uniform heating condition.

On the other hand, the highest temperature excess values were observed in the cases where the non-powered elements were placed at the channel entrance region. However, for distances between plates above 2.5cm, there was no practical difference, in terms of temperature excess, between placing the unheated elements in the channel entrance or exit regions.

It can be concluded that, in terms of electronic thermal design, the uniform heating is the best option, followed by the placement of heated components near the channel entrance, which is more effective for small distances between plates.

6. Acknowledgements

To FAPESP for the financial support and to CENAPAD-SP for computer support.

7. Reference list

- Auletta, A., Manca, O., Morrone, B., Naso, V., 2001, “Heat transfer enhancement by the chimney effect in a vertical isoflux channel”, *International Journal of Heat and Mass Transfer*, Vol.44, pp.4345-4357.
- Avelar, A. C. and Ganzarolli, M. M., 2002, “Natural convection heat transfer in an array of vertical channels with two-dimensional heat sources: uniform and non-uniform plate heating”, *Proceedings of the 9th Brazilian Congress of Thermal Sciences and Engineering - ENCIT 2002*, CD, Caxambu-MG, Brazil.
- Avelar, A. C. and Ganzarolli, M. M., 2003, “Optimum spacing in an array of vertical plates with two-dimensional protruding heat sources cooled by natural convection”, *Proceedings of the 10th Brazilian Congress of Mechanical Engineering*, CD, São Paulo, Brazil.
- Bessaih, R., Kadja, M., 2000, Turbulent natural convection cooling of electronic components mounted on a vertical channel. *Applied Thermal Engineering*, v.20, n.1, p.141-154.
- Campo, A., Manca, O. and Morrone, B., 1999, “Numerical Analysis of partially heated vertical parallel plates in natural convective cooling”. *Numerical Heat Transfer, Part A*, Vol. 36, pp.129-151.
- Fujii, M., Gima, S., Tomimura, T. and Zhang, Z., 1996, “Natural convection to air from an array of vertical parallel plates with discrete and protruding heat sources”, *International Journal of Heat and Fluid Flow*. Vol. 17, pp. 483-496.
- Lee, K., 1994, “Natural convection in vertical parallel plates with an unheated entry or unheated exit”. *Numerical Heat Transfer, Part A*. Vol. 25, pp.477-493.
- Patankar, S. V. and Spalding, D. B. A., 1972, “Calculation procedure for heat, mass and momentum transfer in three-dimensional parabolic flows”. *International Journal of Heat and Mass Transfer*, Vol.15, n.10, pp. 1787-1806.
- Patankar, S. V., Liu, C. H. and Sparrow, E. M., 1977, “Fully developed flow and heat transfer in ducts having streamwise-periodic variations of cross-sectional area”. *Journal of Heat Transfer*, Vol. 99, pp. 180-186.
- Patankar, S. V., *Numerical heat transfer and fluid flow*. New York Publishing Co, 1980.
- Haaland, S. E. and Sparrow, E. M., 1983, “Solutions for the channel plume and the parallel –walled chimney”, *Numerical heat transfer*, Vol. 6, pp. 155-172.
- Wirtz, R. A. and Haag, T., 1985, “Effect of unheated entry on natural convection between vertical parallel plates”, ASME paper 85-WA/HT-14.
- Versteeg, H.K., Malalasekera, W., 1999, “An Introduction to Computational Fluid Dynamics”, Longman, Malaysia, TCP, 1999.